DESIGN OF A NONIMAGING FRESNEL LENS FOR SOLAR CONCENTRATORS

RALF LEUTZ*†, AKIO SUZUKI**,
ATSUSHI AKISAWA* and TAKAO KASHIWAGI*
*Tokyo University of Agriculture and Technology,
Department of Mechanical Systems Engineering
2-24-16 Naka–cho, Koganei–shi, Tokyo 184-8588, Japan
† email ralf@star.cad.mech.tuat.ac.jp, phone/fax +81-42-388-7076
**UNESCO, Bouvin 3.26 SC/EST, 1, rue Miollis, 75732 Paris Cedex 15

Abstract—An optimum convex shaped nonimaging Fresnel lens is designed following the edge ray principle. The lens is evaluated by tracing rays and calculating a projective optical concentration ratio. This Fresnel lens is intended for use in evacuated tube type solar concentrators, generating mid-temperature heat to drive sorption cycles, or provide industrial process heat. It can also be used along with a secondary concentrator in photovoltaic applications.

1 INTRODUCTION

This paper describes the design and optimization of a nonimaging Fresnel lens for the use in a solar thermal collector with low concentration ratio intended to provide the driving heat source for a sorption heat pump cycle, operating on solar heat of 80 $\sim$ 250℃. A Fresnel lens of a geometrical concentration ratio of 1.5 $\sim$ 2 in an evacuated tube type collector offers high optical and thermal performance. The collector is not tracking the sun. A larger Fresnel concentrator with higher concentration ratio could be used for photovoltaic applications. If a secondary concentrator and a diffusor are provided, non–tracking operation is possible, and the irradiance should be well distributed over the photovoltaic panel. The first stage of such a concentrator is represented by the lens, a second stage could be comprised by parabolic shaped walls, and/or a diffuser (to solve the problem of inhomogeneous illumination on the pv–panel). A schematic is given in Fig. 1. Flux concentration in such a system is around 15 $\sim$ 20. The novel nonimaging Fresnel lens offers the advantage of requiring only passive tracking, and seasonal tilt.

Acrylic resin (Polymethylmethacrylate, PMMA) is the preferred lens material having a long lifetime under the sunlight (Rainhart and Schimmel, 1974), being transparent to most of the wavelengths within the solar spectrum, and ensuring cost advantageous mass productibility by means of molding or extrusion.

An optimum shaped Fresnel lens refracts all incident rays within two design angles to the absorber. These so called acceptance angles are arranged perpendicular to each other, spanning the hemisphere. The cross sectional design angle is split into two symmetrical acceptance half angles $\pm\theta$. Perpendicular to the cross section, two acceptance half angles $\pm\psi$ are defined. Two pairs of angles are necessary to account for incident sunlight in both planes, as the sun moves daily and seasonally over the sky. Refraction does happen in both planes.

A schematic of a prism for a Fresnel lens depicting the extreme incident rays in both planes along two acceptance half angles, and their refraction (not to scale) is shown in Fig. 2.

In the last two decades, two classes of Fresnel lenses for use in solar collectors have been proposed. O'Neill (1978) designed a point-focusing (not nonimaging) shaped Fresnel lens with

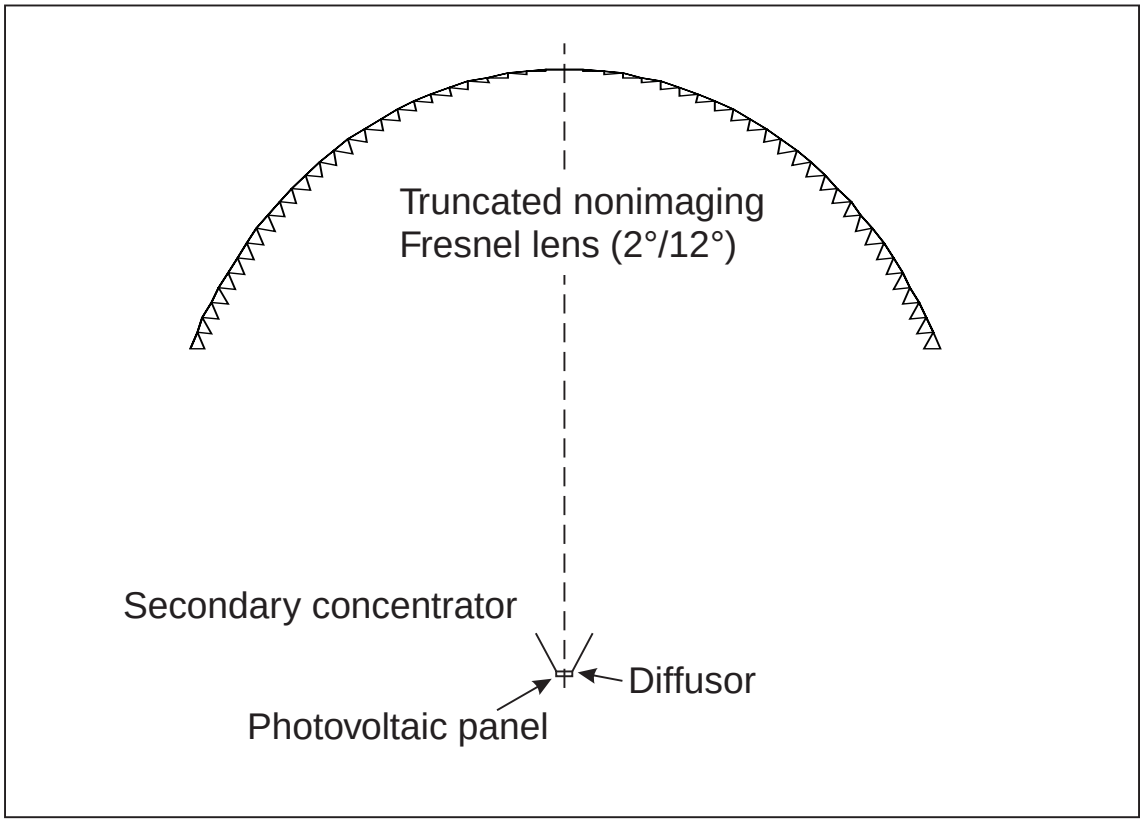

Figure 1: Schematic of truncated nonimaging Fresnel lens with secondary concentrator for application in photovoltaic systems.

high concentration, operating for normal incidence, making tracking inevitable. Kritchman *et al.* (1979a, 1979b) designed nonimaging Fresnel lenses according to the edge ray principle. This principle has been introduced by Welford and Winston (1978) for nonimaging Compound Parabolic Concentrators (CPC), a solar thermal collector developed by Winston (1974) and Rabl (1976). It can be applied to nonimaging lenses.

Secondary concentrators have been proposed by other authors to correct the focal aberrations inherent in a Fresnel lens system. Collares-Pereira *et al.* (1977), and Collares-Pereira (1979) are to be mentioned. A thorough analysis of Fresnel lenses for solar concentration is given by Lorenzo and Luque (1981, 1982), and Lorenzo (1981).

Design approaches in the past have been two-dimensional, as they considered only the cross sectional pair of design angles for developing the lens. A three-dimensional approach takes into account the acceptance half angles for the plane perpendicular to the cross section, and considers additional focal shortening, and allows for simulation of the lens orientation.

2 FRESNEL LENS OPTICS

Fresnel lenses suffer optical problems, both in image quality and focal aberration. Since the lens to be designed here is nonimaging, image quality poses no threat to solar energy collection. A major problem with lenses are focal aberrations which can become severe with large incidence angles.

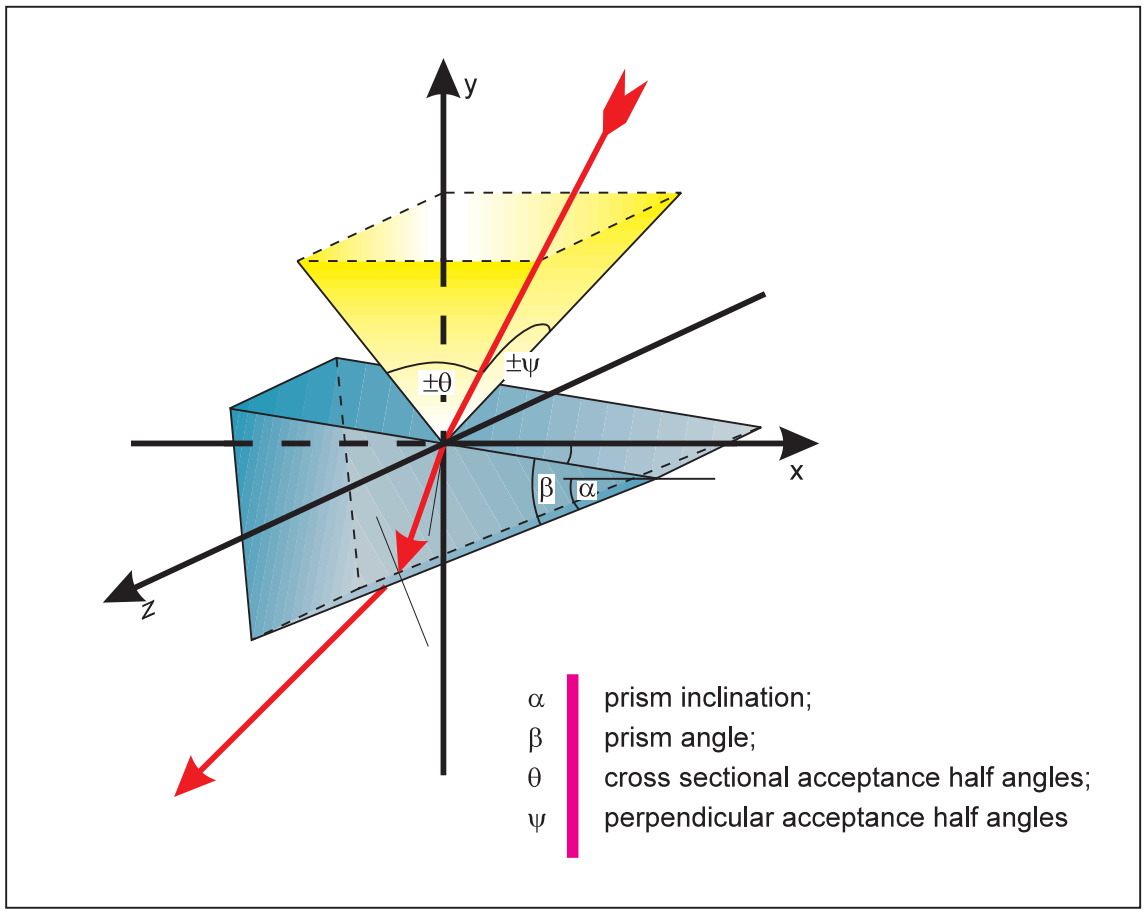

Figure 2: Schematic of prism for Fresnel lens with extreme incident rays along two acceptance half angles, not to scale.

2.1 Nonimaging optics

Contrary to imaging lenses, a nonimaging Fresnel lens does not picture an image of the source in the focal plane. For the collection of the energy of solar rays, photographic accuracy is not necessary. Instead of designing the prisms in order to focus on one point, the prisms are constructed in such a way that refracted rays will hit the absorber at a segment corresponding to the incidence angle, with rays entering at the acceptance half angles reaching the absorber at the very ends. This is the edge ray principle of Welford and Winston (1978). It states that extreme rays entering a concentrating system through an aperture (here: lens surface) must be extreme rays when leaving this system through another aperture (here: receiver), if the achieved optical concentration should be maximal. Since the lens is symmetrically convex shaped, both rays entering the left and the right side can be refracted towards the absorber.

Nonimaging Fresnel lenses of small concentration ratios with acceptance half angles of, for example, cross–sectional $\pm\theta = 30°$, and perpendicular $\pm\psi = 45°$ do not require tracking when set up with East–West orientation with latitude tilt, since θ is greater than the sun's declination caused by seasonal movements of the earth.

2.2 Refraction and reflection

The law of refraction (Snell's law) states that the refracted ray lies in the plane of incidence, and that the sines of the angles between surface normal and incident ray Φ_i, and surface normal and refracted ray Φ_i' are equal (modified by the refractive indices of the first and second materials n and n'):

$$n \sin \Phi_i = n' \sin \Phi_i' \tag{1}$$

The three–dimensional design is best cared for by using vectors representing the incident and refracted rays. A set of equations and constants can be found to calculate both reflection and refraction according to Fig. 3.

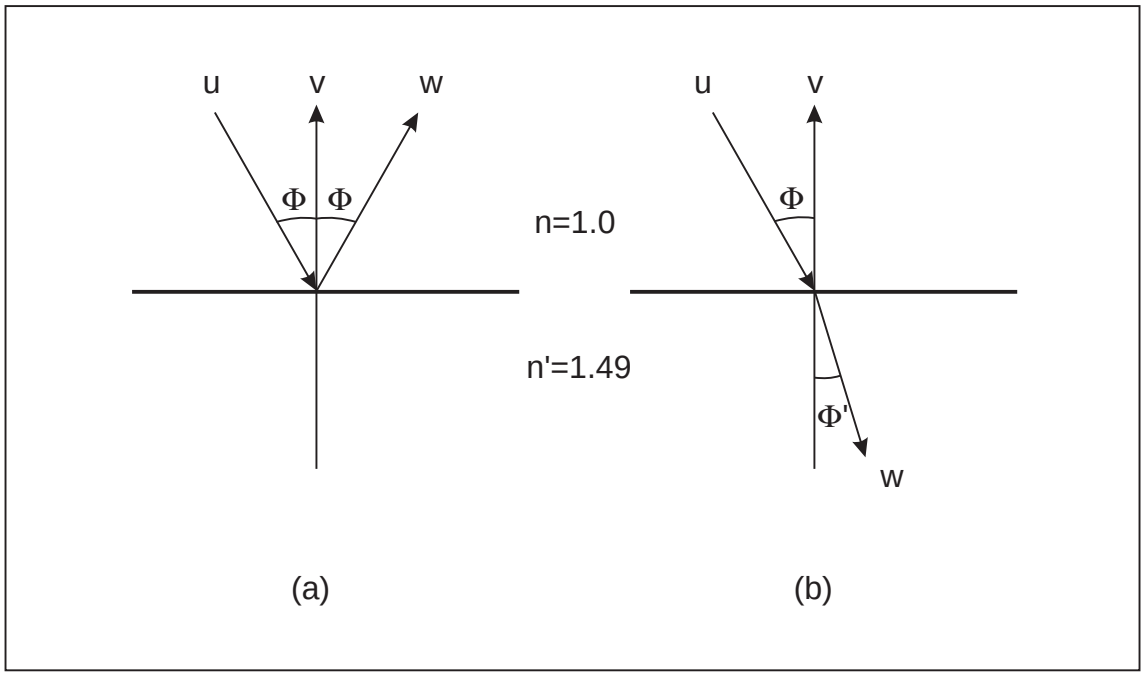

Figure 3: Schematic for reflection (a) and refraction (b) of incident ray on a boundary surface. Two–dimensional view.

$$\begin{aligned} \vec{w}.u &= a\ \vec{v}.u + b\ \vec{u}.u \\ \vec{w}.v &= a\ \vec{v}.v + b\ \vec{u}.v \\ \vec{w}.w &= a\ \vec{v}.w + b\ \vec{u}.w \end{aligned} \tag{2}$$

The factors a and b are given in Tab. 1. Three cases are significant for this evaluation: (i) refraction at the first surface of the prism, (ii) refraction at the second surface of the prism, and (iii) total reflection on the second surface of the prism. The refractive index changes from case (i) to cases (ii, iii) from $n_{acrylic}$ to n_{air}. For the nomenclatura used refer to Fig. 4.

Total reflection is checked, it occurs only when the critical angle $\Phi_c = \Phi_2' < 42.6°$. This value is found for a refractive index of the material (PMMA) $n' = 1.49$, when substituting the angle of refraction in Snell's law with the maximum 90°.

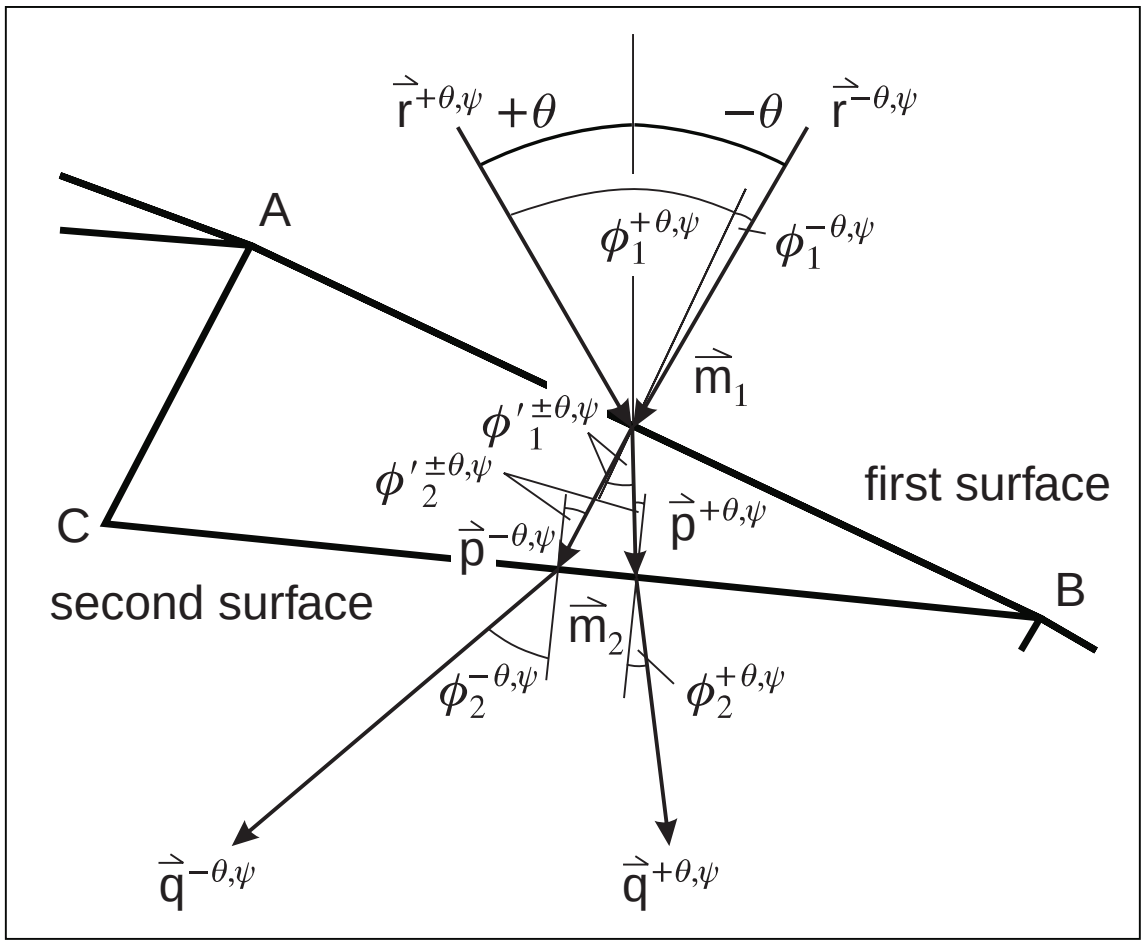

Figure 4: Nomenclature used for the description of reflection and refraction at the prism. The incident rays $\vec{r}_i$, the rays refracted at the first surface $\vec{p}_i$, and the rays refracted at the second surface $\vec{q}_i$ are drawn to scale depending on the extreme acceptance half angles $\pm\theta = \pm 30°$, and $\pm\psi = 45°$. Projection into the cross–sectional plane.

The angles Φ_2' that are not subject to total reflection lie within a cone of rotational symmetry formed around the second surface normal $\vec{m}_2$.

The vector $\vec{p}^{+\theta\psi}$ is used for determination of the prism's tip (point C in Fig. 4). The tangent of the vector's projection into the cross–sectional plane represents the slope of the vector. Point C can be calculated when the slopes and equations for the lines $\overline{AC}$ and $\overline{BC}$ are known.

Reflection losses of a Fresnel lens are minimized by using minimum deviation prisms, i.e. prisms where the angle between the incidence ray and the first surface normal is the same as the one between the transmitted ray and the second surface normal. A mathematical proof for minimum deviation at the prism can be found in Born and Wolf (1989).

2.3 Focal shortening

Increasing focal length shortening and off axis shift becomes severe with greater incidence angles. There are cross sectional θ and perpendicular ψ aberrations which depend on the respective angle of incidence, and the refractive index of the lens' material n. Off-axis lateral θ-aberrations happen in the cross sectional plane, resulting in the focus shifting on a curve left or right, and

Table 1: Factors for calculating reflection and refraction at the prism. $n' = 1.49$, refractive index of PMMA.

Case	Factor a	Factor b
Refraction at the prism's first surface	$\frac{1}{n'}$	$-\cos\Phi_1' + \frac{1}{n'}\cos\Phi_1$
Refraction at the prism's second surface	n'	$-\cos\Phi_2' + n'\cos\Phi_2$
Reflection at the prism's second surface	1	$-2\cos\Phi_2$

up. Longitudinal ψ-aberrations in the perpendicular plane foreshorten the back focal distance. The factors describing foreshortening in an imaging refractive concentrator are (Meinel and Meinel, 1976)

$$\ell_\theta \cong 1 - n\,(1 - \cos\,(\theta/n)) \tag{3}$$

and for off-axis longitudinal ψ-aberrations in the perpendicular plane

$$\ell_\psi = \sqrt{1 - (1/n^2)\sin^2\psi} \tag{4}$$

Unfortunately, these equations for focal shortening as given do not hold true for Fresnel lenses. For a nonimaging Fresnel lens, the resulting curve of focal areas does not lie on the cross section of the Petzval surface, as it does for a single lens. Thus, we cannot analytically find the off-axis shift in order to size and position the absorber. Instead, minimum deviation prisms are individually positioned over an absorber of given width according to the edge ray principle. The problem of focal shortening is eased in convex shaped Fresnel lenses, as the inclination of prisms in the cross sectional plane partly adjusts for incidence angles that would be resulting in strong foreshortening on a flat lens.

The refractive index of a material depends on the wavelength of the incident light. Dispersion has to be accounted for at high concentration ratios and when designing imaging devices. Lorenzo (1981) finds chromatic aberrations in Fresnel lenses with acceptance half angles greater than 5° to be negligible. The refractive index for acrylic varies from $n_{red} = 1.485$ to $n_{blue} = 1.495$. Using $n = 1.49$ in the design of a Fresnel lens of low concentration is reasonable, while dispersion might account for part of the edge rays missing the absorber.

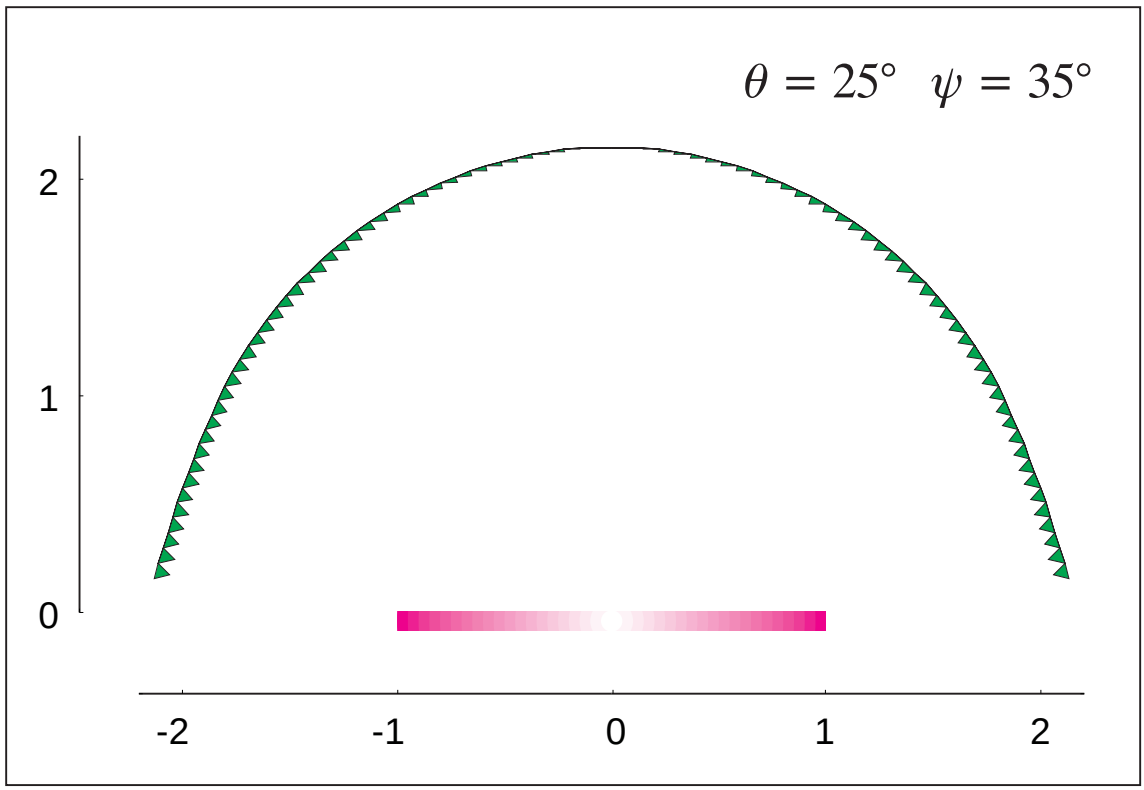

Figure 5: Optimum nonimaging Fresnel lens, concentration ratio around 2.1, acceptance half angles $\theta = 25°$, $\psi = 35°$. Absorber half width $d = 1$.

3 FRESNEL LENS DESIGN

A symetrical convex shaped Fresnel lens is designed. As opposed to other nonimaging concentrators, the three–dimensional design of an optimum shaped Fresnel lens according to the edge ray principle is defined by seven parameters:

- The cross–sectional acceptance half angle pair $\pm\theta$.
- The perpendicular acceptance half angle pair $\pm\psi$. Other nonimaging concentrators, like the reflecting CPC, can be designed without having to consider the perpendicular acceptance half angle ψ, which is needed for the refractive case.
- The angle ω that devides the aperture of the lens into equal segments (like the spokes of a wheel), and subsequently defines the pitch Δx by which the projected width of a prism is defined. This also limits the number of prisms constituting the lens.
- The prism inclination α.
- The prism angle β.
- The average refractive index of the material n.
- An error margin ΔE.

Direct solar radiation reaching the outer surface of the lens at an angle smaller or equal to the acceptance half angles will, according to the edge ray principle, be refracted to the absorber. The height f of the lens above the absorber can be expressed as

$$f = d/\tan\theta \tag{5}$$

where d is the reference length and width of half the absorber. From this reference point, the position and angles of the first prism to the right of the center of the lens are determined. All succeeding prisms start where the previous one was finalized. Initial angles for the adjacent prisms are the final ones of the previous prism. Only the right side of the lens is determined. Since the lens is two–dimensional, the left side of the lens is mirrored from the right side.

The width of a prism is decided by the lens designer by setting the angle ω. Like the spokes of a wheel, the next prism will be set further to the right and further down towards the absorber level.

For a first prism, the prism inclination angle α is set to zero. With two directions of incidence ($+\theta\psi$, $-\theta\psi$), two values for the prism angle β are found. Both angles are determined with Newton's method in infinity loops. Imagine the result for the first iteration with $\alpha = 0$ does not yield two prism angles β_1 and β_2 for which

$$|\beta_1 - \beta_2| < \Delta E \tag{6}$$

where ΔE is the error margin, or a confidence level. If the condition in Eqn. 6 is not fulfilled, the program enters into the infinity loop, and the prism inclination angle α is decreased by $\Delta\alpha = 1°$. Two new values (one for each direction of incidence) for the prism angle α are found. If the condition of Eqn. 6 remains unfulfilled, Newton's method is employed to find a new value for the prism inclination angle α. After a few iterations, the prism inclination angle α is set; the criterion of Eqn. 6 has been fulfilled.

A procedure very similar to the one outlined above for the optimization of the prism inclination angle α is employed for finding the optimum prism angle β. This time the condition to fulfill describes the position of the prism relative to the absorber in its relation to the direction of the refracted rays $\vec{q}^{+\theta\psi}$ and $\vec{q}^{-\theta\psi}$. These relations are shown in Fig. 6.

The prism position over the absorber is determined via two positioning vectors which describe the center point of the prism bottom in its position to either end of the absorber. Incidence on the prism from the left and right sides should hit the absorber after refraction within the limits of the right or the left end of the absorber, respectively. The prism has to be designed in such a way, that this edge ray principle can be maintained. Thus, if the vector pair $\vec{q}^{-\theta\psi}$ and $\vec{d}^{-\theta\psi}$ as well as the vector pair $\vec{q}^{+\theta\psi}$ and $\vec{d}^{+\theta\psi}$ can be kept parallel, all rays leaving the prism after refraction will hit the absorber within its outer limits. It has to be noted that the vectors $\vec{q}$ in Fig. 6 are plotted to scale, the vectors $\vec{d}$ are not.

The optimization criterion for Newton's method and the setting of the prism angle β (not to mention the setting of the prism inclination angle α in the outer loop) is

$$\left| \frac{\vec{q}.x}{\vec{q}.y} - \frac{\vec{d}.x}{\vec{d}.y} \right| < \Delta E \tag{7}$$

Only when this condition (Eqn. 7) is satisfied, the infinity loop is broken, and the prism angle is set. This supplies a value for the outer loop where the condition of Eqn. 6 has to be met for the finish of the prism under design. It should be noted that the condition of Eqn. 7 is the projection onto the plane of the paper, and includes the three–dimensional calculation of $\vec{q}$.

When the prism under consideration is rather low at the side of the lens, close to the absorber level, the prism inclination angle α becomes relatively large. With an even greater prism angle β,

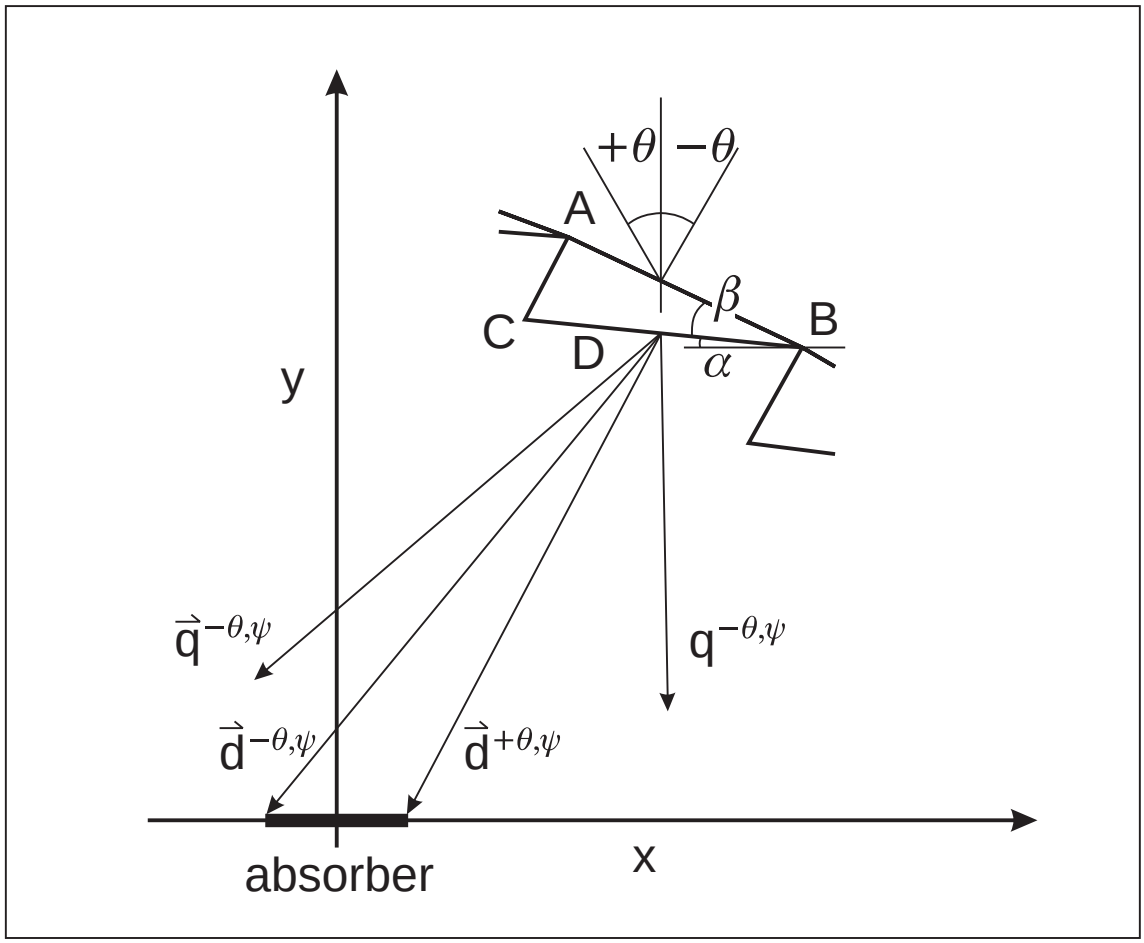

Figure 6: Evaluating the prism position relative to the absorber. Refracted edge rays for incidence from both sides, and depending on $\pm\psi$ (vectors $\vec{q}^{+\theta\psi}$ and $\vec{q}^{+\theta\psi}$) are compared with the prism position vectors relative to either end of the absorber $\vec{d}^{+\theta\psi}$ and $\vec{d}^{+\theta\psi}$. The vectors $\vec{q}$ are plotted to scale, the vectors $\vec{d}$ are not. Projection into cross–sectional plane.

the incidence coming at a maximum angle $+\theta$ from the left side, could be shaded by a previous prism. Shading happens when the scalar product of the incident ray and the prism face normal becomes negative. If

$$\vec{r} \bullet \vec{m}_1 < 0 \tag{8}$$

is true, then the infinity loop determining the optimum prism inclination angle α is broken, and the last value for α is kept constant and used for all subsequent prisms. The prism angle β, however, is increased further in order to optimize the prism for incidence $-\theta$ from the right side of the lens, and for the perpendicular incidence ψ.

The symmetry in the incidence angles $\pm\theta$ and ψ determining the vectors $\vec{d}^{\pm\theta\psi}$ reaching the edges of the symmetrical absorber, as well as the quasi–symmetry in splitting the design of the prism into the calculation of two dependent angles α and β results in the creation of prisms that are close to minimum deviation prisms.

Of course, one prism can have only one angle of minimum deviation, but the design described here yields paths for both edge rays that are reversible. For the maximum angle of incidence on the first surface from the left side $\phi_1^{+\theta\psi}$, an angle of refraction on the second surface $\phi_2^{+\theta\psi}$ is recorded, where the latter approximately coincides with the the angle of maximum incidence

from the right side $\phi_1^{-\theta\psi}$, and the former roughly equals the angle of refraction for incidence from the right side on the second surface $\phi_2^{-\theta\psi}$.

Although minimum deviation happens only for one angle of incidence on each prism, symmetrical paths and the principle of the reversibility of light are the basic concepts of minimum deviation, the 'reversible' prisms described here are to be called minimum deviation prisms.

A cross sectional view of a Fresnel lens designed this way with the acceptance half angles $\theta = 25°$ and $\psi = 35°$ is shown in Fig. 5. The left side of the lens is a symmetrical copy of its right side.

At an receiver half width of $d = 1$ the actual geometrical concentration ratio is readily available as 2.1 on the x-axis. The theoretical geometrical concentration ratio is

$$C = \frac{1}{\sin\theta} \tag{9}$$

For the examplatory lens with the acceptance half angles $\theta = 25°$ and $\psi = 35°$, $C = 2.37$. The elevation angle ψ leads to a higher concentration ratio $C_{3D} = 1/(\sin\theta\ \sin\psi)$, but limits the acceptance of radiation from perpendicular directions. We are considering (projected) lengths instead of areas, and are inclined to using the concentration ratio $C_{2D} = 1/\sin\theta$.

The idea behind this way of proceeding becomes more clear when comparing the Fresnel lens with a CPC collector. Imagine the CPC to be short, i.e. having a perpendicular cut–off angle due to shading from both ends of the tube, which has to be considered during evaluation of the CPC's performance. Likewise, the perpendiclar angle ψ in the lens is an angle cutting off solar rays, rather than an angle useful in concentration. The elevation angle should be understood as limiting the performance of the refractive system.

The flow chart of the 'C' program used for the design of the optimum shaped lens is pictured in Fig. 7.

4 LENS EVALUATION

After the lens is designed the second part of the simulation evaluates its optical properties. For combinations of angles 180° over the cross sectional plane, and for 90° (since being symmetrical) over the plane perpendicular to it, incidence rays are generated for each prism. Their paths are followed, and unused prism tips and blocking losses are calculated by intersection of the rays with the prism's front and bottom. Rays missing the absorber also contribute to optical losses. This procedure is called ray tracing and leads to quantification of losses.

4.1 Losses

Solar rays hitting a prism at angles other than the design angles will be refracted towards the prism bottom. At the right half of the lens, the rays will intercept the bottom not at the prism tip, but instead left (imaginary) or right of it. Both cases lead to the loss of solar radiation, for incidence angles greater than the design angles the rays will be reflected and refracted at the prism back, partly not reaching the absorber, or in the second case, for angles smaller than the design angles, the rays will be refracted to the absorber, but leave a part of the prism tip unused.

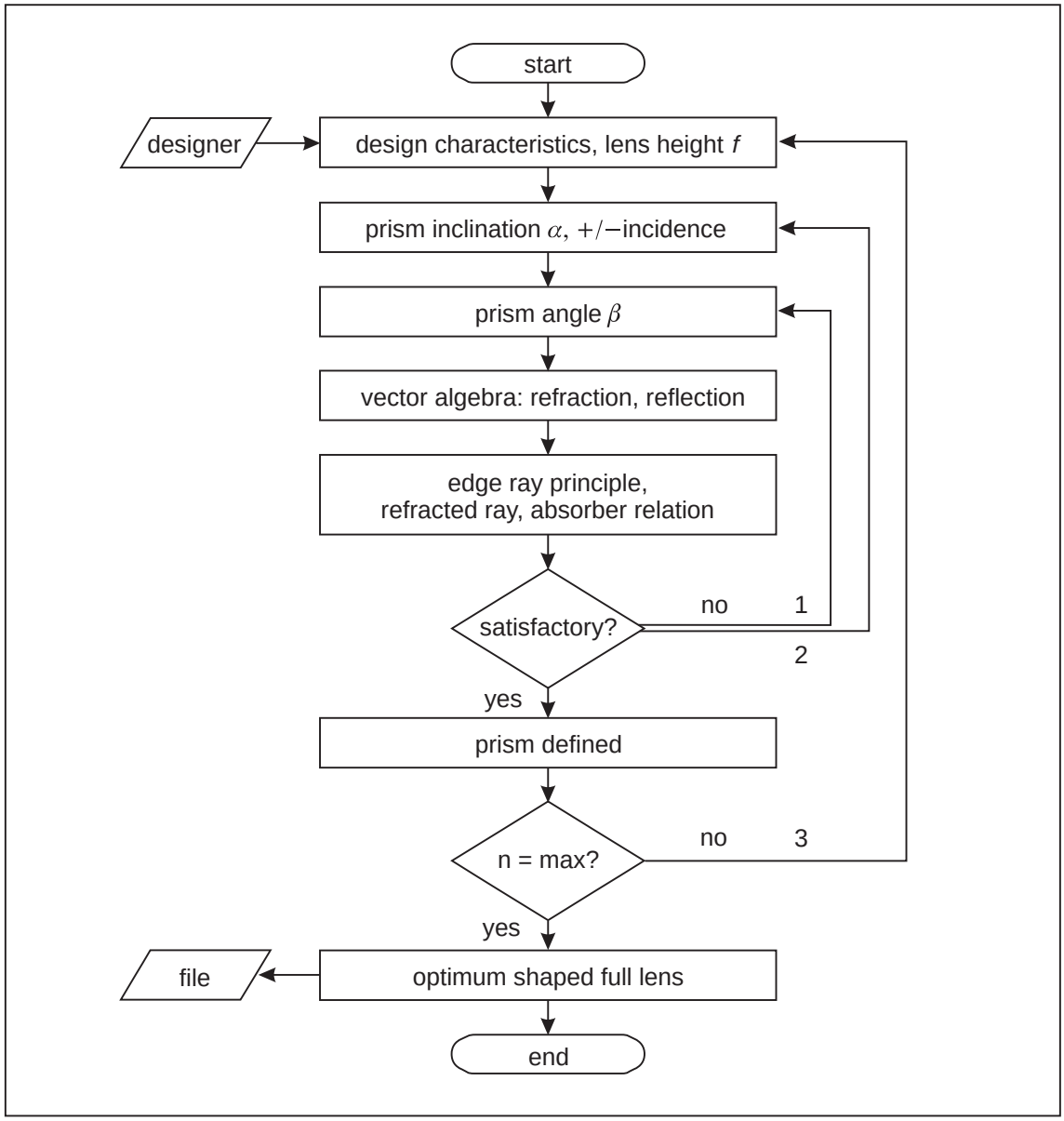

Figure 7: Flow chart of optimum lens calculation, n = number of prism.

Outermost refracted rays will, except for the case of incidence at the design angle from the right for the right side of the lens (and from the left for the left side of the lens), be blocked at the adjacent prism's back. Only a fraction of the rays will be reflected from there towards the absorber. These losses are termed blocking losses.

A simulation moving the prism tip horizontally towards the outside of the lens to minimize blocking losses showed mixed results. Gains are observed for prisms in the upper part of the lens, but the increase in collected energy is not significant.

Focal forshortening is responsible for losses occuring at the lens for incidence angles $|\psi_{in}| < |\psi|$, at $|\theta_{in}| = |\theta|$). For the perpendicular incidence $|\psi_{in}| > 0$ the focal plane of the lens moves towards the prisms (upwards when seen from the absorber). Imagine the prism in Fig. 8 on the right side of the lens. When ψ_{in} becomes smaller than the acceptance half angle ψ, the focal plane moves downward, and some of the rays miss the absorber on the right.

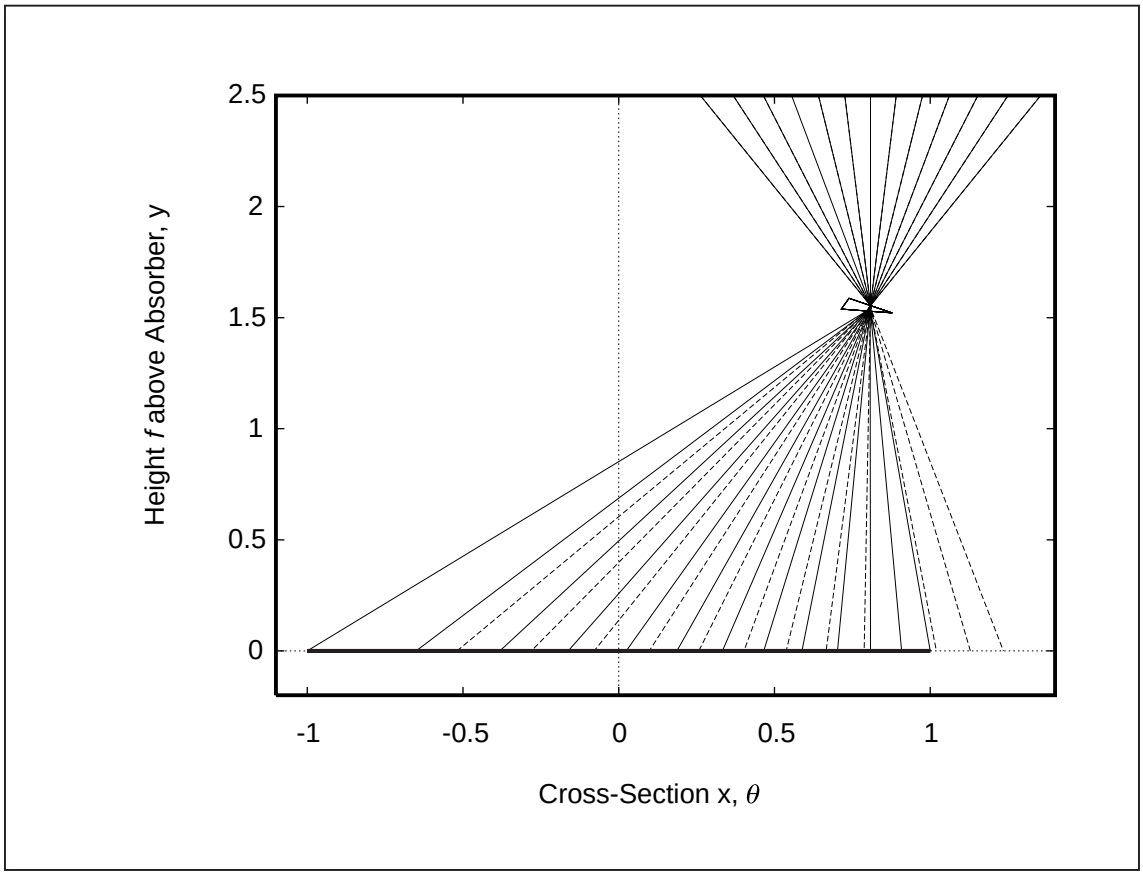

Figure 8: Tracing rays within the design angles $\theta = \pm 30°$, $\psi = \pm 45°$. The full lines depict rays $-30° \leq \theta_{in} \leq +30°$ and $\psi_{in} = \psi = 45°$. The dashed lines are for $-30° \leq \theta_{in} \leq +30°$ and $\psi_{in} = 0°$, at $\psi = 45°$. Due to focal shortening, the rays incident at the greater incidence angles ψ_{in} fill out the absorber, while some rays in the second case miss. The absorber or exit aperture, is no Lambertian light source for three–dimensional incidence, and the optimum nonimaging Fresnel is not an ideal concentrator.

4.2 Concentration ratios

For the nonimaging Fresnel lens a geometrical concentration ratio is calculated for combinations of incidence angles in 5°-steps. The geometrical concentration ratio for a lens with $\theta = 25°$ and $\psi = 35°$ at normal incidence is calculated to 2.37, shown in Figs. 5 and 9 as the ratio between 'thickness' of the incident radiation (measured between the outermost rays for a lens that would reach the absorber level) and the absorber width. Stating a concentration ratio for a shaped Fresnel lens is an ambiguous concept as one could also define a concentration ratio calculated as the ratio of the horizontal projection of the incident beam and the receiver width. The latter concept resembles the one used for describing the edge ray principle, as this is based on horizontal apertures, like at a CPC. For incidence angles close to 90°, however, this concentration ratio becomes infinity. Nevertheless, for reasons of comparability, this concept is preferred here. The discussion follows the concepts of concentration ratios outlined by Welford and Winston (1989).

It is emphasized to describe the nonimaging lens in terms of the incoming light reaching the absorber. This value, called an optical efficiency, incorporates geometrical losses due to unused prism tips and blocking at adjacent prisms' backs, absorber misses, and optical losses (transmissivity) accounting for first order reflection. Following the concept of geometrical and projective concentration the optical efficiency is calculated for combinations of incidence angles, as seen in Fig. 10. Naturally, the optical efficiency is independent of the way of calculating the

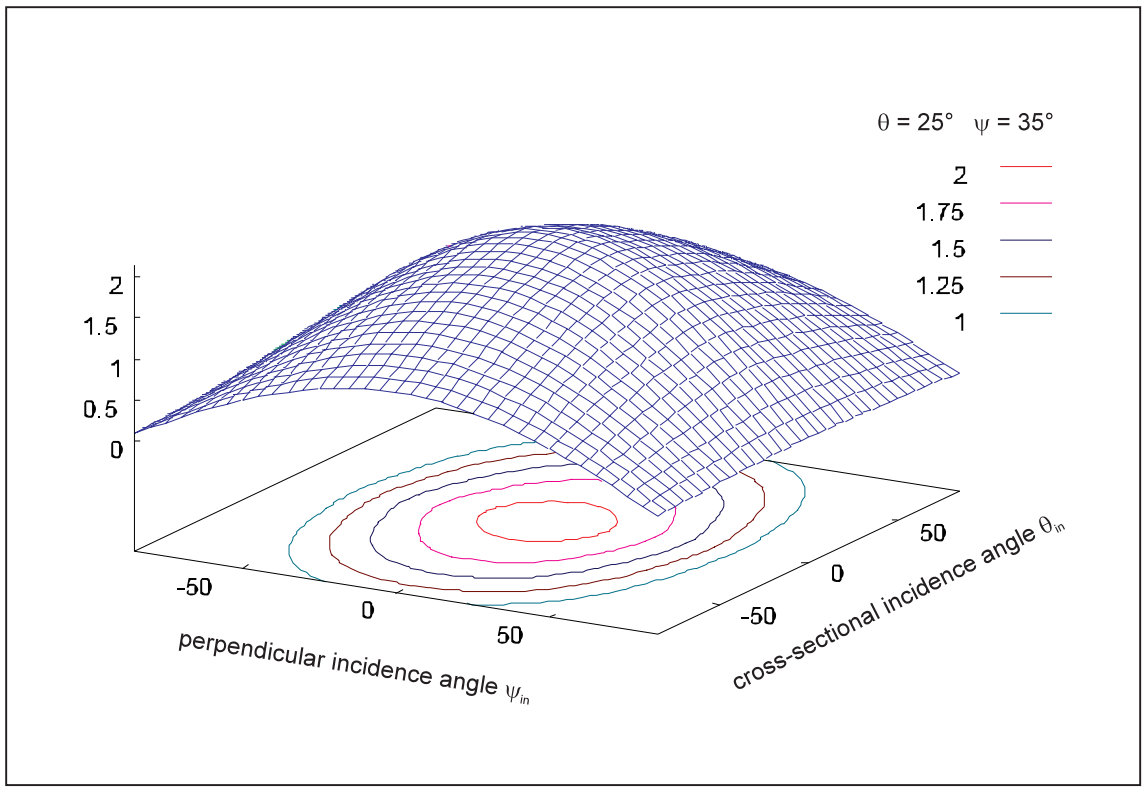

Figure 9: Geometrical concentration ratio of a nonimaging Fresnel lens with acceptance half angles $\theta = 25°$, $\psi = 35°$, combinations of incidence angles, ψ_{in} and θ_{in}.

concentration ratio. The result shows a peak of optical efficiency in the range of the design angles at $\theta_{inc} = 20°$ and $\psi_{inc} = 35 \sim 40°$. The variation from the design angles can be explained with the previously mentioned absorber misses. Remarkable in Fig. 10 is the wide range of high optical efficiency in spite of blocking losses. Its sharp drop after exceeding the design angles is a typical feature of nonimaging concentrators due to their design according to the edge ray principle: incidence at angles greater than the design angles generally misses the absorber.

The optical efficiency multiplied with the geometric, or the projective concentration ratio results in the optical concentration ratio of the lens. The optical concentration can also be understood as ratio between radiation intensity with concentrator by radiation intensity without concentrator. It is again calculated for combinations of angles of incidence. The projective optical concentration is pictured in Fig. 11. Incorporated for comparison is the same lens truncated at half height above the absorber.

Nonimaging concentrators like the CPC or this Fresnel lens can be truncated at half height ($f_{trunc} = 1/2f$). The parabolic mirrors or the prisms are cut with minor impact on concentrator performance but significant cost reduction.

Even for the truncated lens, the range of incidence angle combinations giving almost uniform optical concentration is surprisingly wide before sharply dropping. Calculated with the projective concentration ratio, this range is slightly higher, and its maximum is shifted towards greater angles of incidence. Lenses designed with greater acceptance half angles further widen this plateau.

The optical concentration ratio resembles an energetic efficiency. It makes the performance of a lens comparable to other solar concentrators' performances. Also, this ratio can be integrated in an overall efficiency of the collector (multiplying it with the absorber's efficiency), and into system evaluations.

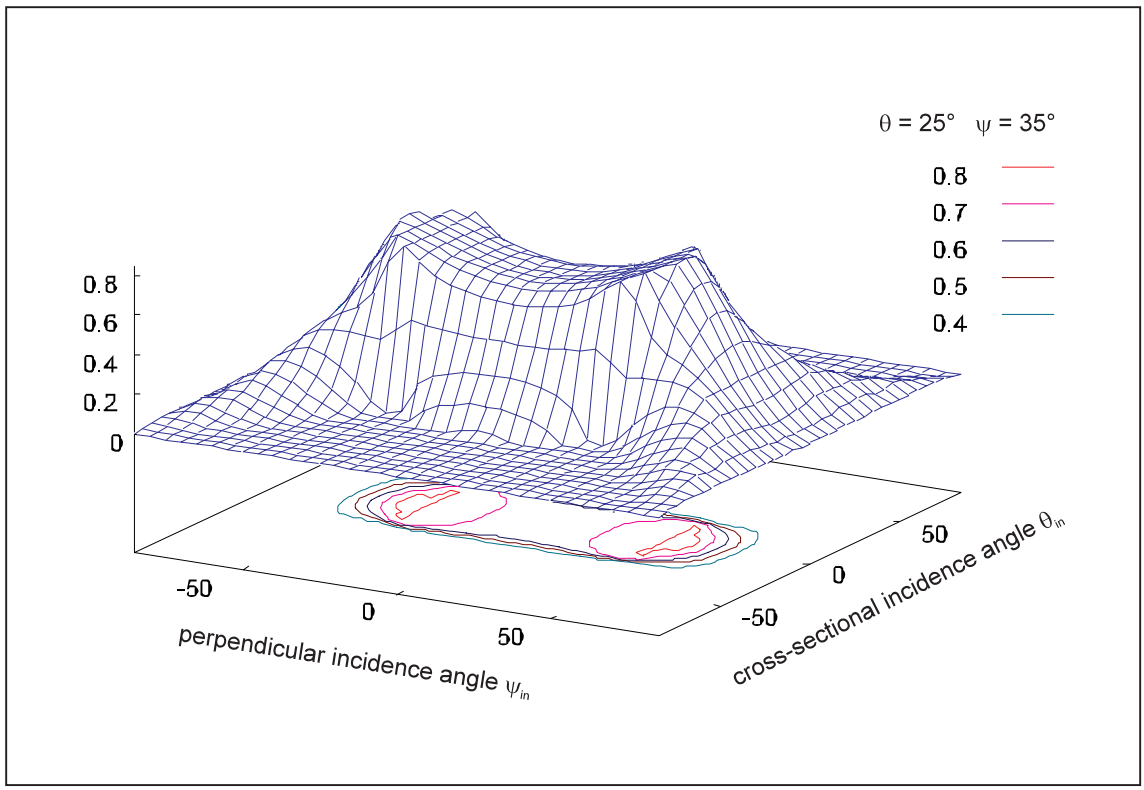

Figure 10: Optical efficiency of an optimum nonimaging Fresnel lens, $\theta = 25°$ and $\psi = 35°$, incidence angles ψ_{in} and θ_{in}.

Values for average efficiencies over the acceptance angles of the lens are given in Tab. 2. The values for optical performance are expected to increase once the lens is optimized under a radiation model, i.e. taking into account the direction and strength of incoming rays when optimizing the position of the prisms' tips.

Said Table 2 also illustrates that it should make sense to truncate the lens at half height above the absorber. Performance values are not seriously affected.

4.3 Nonideal concentration

A concentrator is called 'ideal' when all rays entering the first aperture of the concentrator system within two pairs of acceptance half angles θ and ψ are exiting through the second aperture of the concentrator system over a solid angle (Winston, 1989). If the light source is Lambertian, or ideal, and being characterized by constant flux over all directions, the second aperture (the absorber) must equal a Lambertian radiator if the concentrator should be called ideal. The sun is an almost ideal radiator, but the absorber of the nonimaging Fresnel lens is not.

The two–dimensional Fresnsl lens concentrator ($\psi = 0$) is approaching the status of being ideal due to the symmetry of the lens, variations in flux from the left side are countered by a similar, but mirrored flux characteristic from the right side of the lens. The cross–section of the absorber is completely filled out with uniform radiation.

However, if incidence from $0 \leq \psi_{in} < \psi$ is considered in the case of a three–dimensional design ($\psi \neq 0$, $\pm\theta = constant$), like in Fig. 8, the absorber no longer is covered by uniform flux. Focal shortening happens in both the cross–sectional, and in the perpendicular direction of

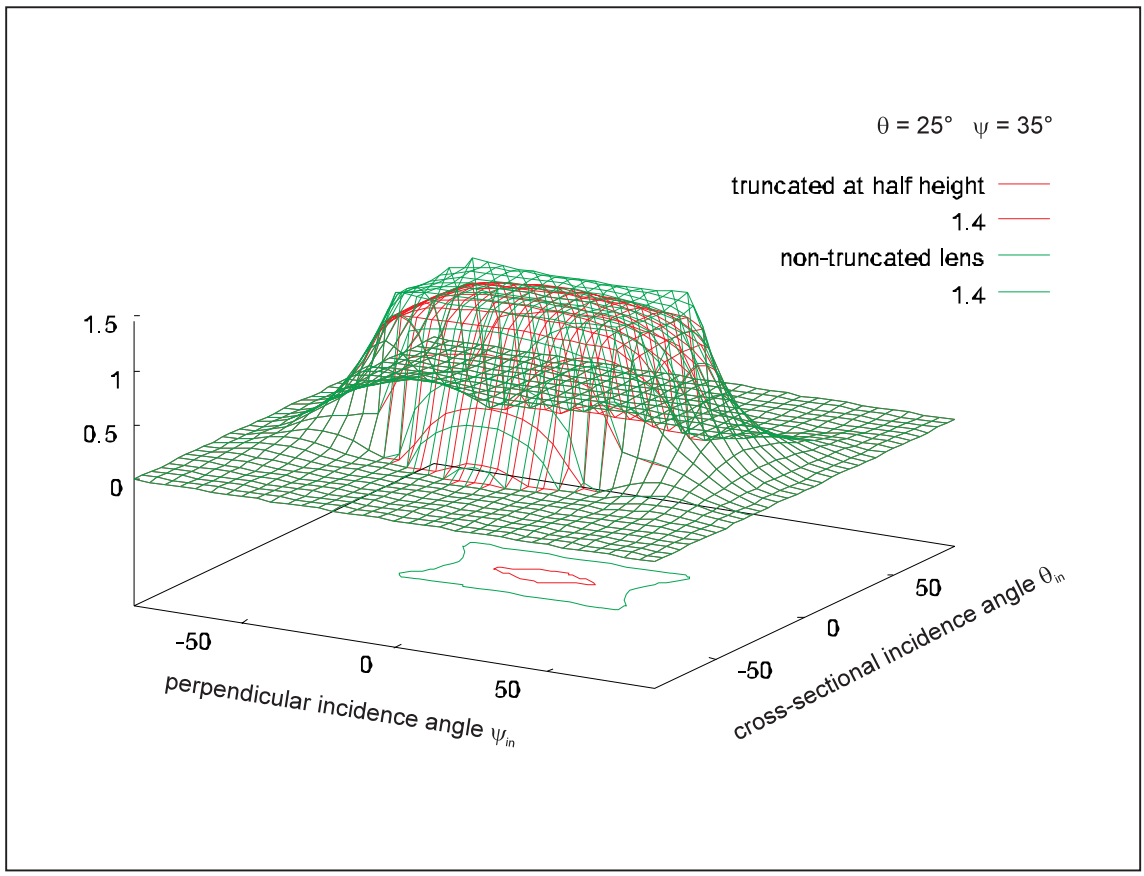

Figure 11: Optical concentration ratio based on the projective concentration ratio of a nonimaging Fresnel lens with acceptance half angles $\theta = 25°$, $\psi = 35°$, incidence angles ψ_{in} and θ_{in}. The same lens is truncated at half height above the absorber for comparison, and shown as inner grid along with the center contour line.

incidence. When the perpendicular incidence angle is smaller than the perpendicular acceptance half angle, the focal plane moves from a position found for the perpendicular design angle further down below the lens. Since the prism in Fig. 8 is located in the right part of the lens, some rays smaller than ψ are missing the absorber (rightmost dashed lines in Fig. 8).

Another reason for not being able to call the Fresnel lens ideal is the total reflection on the outer surface of the lens for prisms towards the absorber level. This is a design inherent problem and limits the performance of the first aperture.

For small perpendicular acceptance half angles ($\psi \to 0$), and using infinitely small prisms, the lens becomes ideal.

5 CONCLUSIONS

An optimum convex shaped Fresnel lens is designed

- according to the edge ray principle;
- in three dimensions, accounting for incidence in the cross sectional, and in the perpendicular plane;
- with minimum deviation prisms for reduced total reflection, and minimum dispersion.

Table 2: Average efficiency ratios of two exemplatory nonimaging Fresnel lenses over their respective acceptance half angles. 'Truncated' stands for the truncation of the lens at half height over the absorber. η: optical efficiency, C: geometrical concentration ratio, η_C: projective optical concentration ratio.

Lens (θ, ψ)	η	C	η_C
2, 12	0.64	21.40	13.67
truncated	0.69	19.04	13.22
30, 45	0.63	1.65	1.15
truncated	0.72	1.36	1.08

Not included in the design for reasons of insignificance or simplicity are effects of chromatic aberration, multiple reflection, absorptance in the lens material, and forms of optical distortion other than deviation.

The Fresnel lens is evaluated by ray tracing. It is made comparable to other solar collectors by an projective optical concentration ratio. The optimum nonimaging Fresnel lens of finite size is not an ideal concentrator. For the case of three–dimensional design, the absorber does not become a Lambertian radiator. For the theoretical case of two–dimensional design ($\psi = 0$), and infinitely small prisms, the lens approaches the ideal.

The nonimaging Fresnel lens can be operated stationary. Acceptance half angle pairs related to small concentration ratios do not require the concentrator to track the sun.

Tip moving to minimize blocking losses lead to insignificant increase in optical efficiency. Truncation at half height reduces the performance of the lens significantly enough to consider the use of a full lens, given the low cost of the acrylic material and lens production.

In the future the lens' performance will be evaluated under an insolation model to find the design angles of the optimum lens for any location on earth, before it will be tested in an evacuated tube type collector providing heat for sorption cycles, or as part of a two–stage concentrator for photovoltaic arrays. For both applications, the lens should have technical and economical potential.

REFERENCES

M. Born, E. Wolf (1989) Principles of Optics, 6.ed., Oxford

M. Collares–Pereira, A. Rabl, R. Winston (1977) Lens–Mirror Combinations with Maximal Concentration; *Applied Optics* **16**, 10, 2677-2683

M. Collares–Pereira (1979) High Temperature Solar Collector with Optimal Concentration: Non–

Focusing Fresnel Lens with Secondary Concentrator; *Solar Energy* **23**, 409-420

E. M. Kritchman, A. A. Friesem, G. Yekutieli (1979a) Efficient Fresnel Lens for Solar Concentration; *Solar Energy* **22**, 119-123

E. M. Kritchman, A. A. Friesem, G. Yekutieli (1979b) Highly Concentrating Fresnel Lenses; *Applied Optics* **18**, 15, 2688-2695

E. Lorenzo, A. Luque (1982) Comparison of Fresnel Lenses and Parabolic Mirrors as Solar Energy Concentrators; *Applied Optics* **21**, 10, 1851-1853

E. Lorenzo, A. Luque (1981) Fresnel Lens Analysis for Solar Energy Applications; *Applied Optics* **20**, 17, 2941-2945

E. Lorenzo (1981) Chromatic Aberration Effect on Solar Energy Systems using Fresnel Lenses; *Applied Optics* **20**, 21, 3729-3732

A. Luque (1989) Solar Cells and Optics for Photovoltaic Concentration, Bristol

A. B. Meinel, M. P. Meinel (1976) Applied Solar Energy—An Introduction, Reading

M. J. O'Neill (1978) Solar Concentrator and Energy Collection System; United States Patent 4069812

A. Rabl (1976) Optical and Thermal Properties of Compound Parabolic Concentrators; *Solar Energy* **18**, 479-511

L. G. Rainhart, W. P. Schimmel (1975) Effect of Outdoor Aging on Acrylic Sheet; *Solar Energy* **17**, 259-264

W. T. Welford, R. Winston (1989) High Collection Nonimaging Optics, San Diego

R. Winston (1974) Principles of Solar Concentrators of a Novel Design; *Solar Energy* **16**, 89-95